7-14-2017

Physiological Evidence for Isopotential Tunneling in the Electron Transport Chain of Methane-Producing Archaea

Nikolas Duszenko

Nicole R. Buan

AMERICAN SOCIETY FOR MICROBIOLOGY | Applied and Environmental Microbiology®

PHYSIOLOGY

Physiological Evidence for Isopotential Tunneling in the Electron Transport Chain of Methane-Producing Archaea

Nikolas Duszenko, Nicole R. Buan

Department of Biochemistry, University of Nebraska, Lincoln, Nebraska, USA

ABSTRACT Many, but not all, organisms use quinones to conserve energy in their electron transport chains. Fermentative bacteria and methane-producing archaea (methanogens) do not produce quinones but have devised other ways to generate ATP. Methanophenazine (MPh) is a unique membrane electron carrier found in *Methanosarcina* species that plays the same role as quinones in the electron transport chain. To extend the analogy between quinones and MPh, we compared the MPh pool sizes between two well-studied *Methanosarcina* species, *Methanosarcina acetivorans* C2A and *Methanosarcina barkeri* Fusaro, to the quinone pool size in the bacterium *Escherichia coli*. We found the quantity of MPh per cell increases as cultures transition from exponential growth to stationary phase, and absolute quantities of MPh were 3-fold higher in *M. acetivorans* than in *M. barkeri*. The concentration of MPh suggests the cell membrane of *M. acetivorans*, but not of *M. barkeri*, is electrically quantized as if it were a single conductive metal sheet and near optimal for rate of electron transport. Similarly, stationary (but not exponentially growing) *E. coli* cells also have electrically quantized membranes on the basis of quinone content. Consistent with our hypothesis, we demonstrated that the exogenous addition of phenazine increases the growth rate of *M. barkeri* three times that of *M. acetivorans*. Our work suggests electron flux through MPh is naturally higher in *M. acetivorans* than in *M. barkeri* and that hydrogen cycling is less efficient at conserving energy than scalar proton translocation using MPh.

IMPORTANCE Can we grow more from less? The ability to optimize and manipulate metabolic efficiency in cells is the difference between commercially viable and nonviable renewable technologies. Much can be learned from methane-producing archaea (methanogens) which evolved a successful metabolic lifestyle under extreme thermodynamic constraints. Methanogens use highly efficient electron transport systems and supramolecular complexes to optimize electron and carbon flow to control biomass synthesis and the production of methane. Worldwide, methanogens are used to generate renewable methane for heat, electricity, and transportation. Our observations suggest *Methanosarcina acetivorans*, but not *Methanosarcina barkeri*, has electrically quantized membranes. *Escherichia coli*, a model facultative anaerobe, has optimal electron transport at the stationary phase but not during exponential growth. This study also suggests the metabolic efficiency of bacteria and archaea can be improved using exogenously supplied lipophilic electron carriers. The enhancement of methanogen electron transport through methanophenazine has the potential to increase renewable methane production at an industrial scale.

KEYWORDS archaea, *Escherichia coli*, *Methanosarcina*, bioenergetics, electron transport, membrane biophysics, methanogens, methanophenazines, phenazines, quinones

Received 26 April 2017 **Accepted** 30 June 2017

Accepted manuscript posted online 14 July 2017

Citation Duszenko N, Buan NR. 2017. Physiological evidence for isopotential tunneling in the electron transport chain of methane-producing archaea. Appl Environ Microbiol 83:e00950-17. https://doi.org/10.1128/AEM.00950-17.

Editor Harold L. Drake, University of Bayreuth

Address correspondence to Nicole R. Buan, nbuan@unl.edu.

The question of how cells obtain energy to grow is fundamental to biology. There are several ways cells metabolize substrates to produce energy in the form of ATP, such as by coupling thermodynamically favorable reactions to the production of a chemiosmotic gradient, substrate-level phosphorylation, and transmembrane cycles, etc. (1–10). Among the interesting organisms that can grow with very little ATP yield are methane-producing archaea (methanogens). Methanogens grow by reducing carbon substrates to methane gas in a process known as methanogenesis (11). Methanogens are strict anaerobes found in a wide range of natural habitats, from freshwater lake sediment to deep sea hydrothermal vents. In these environments, end products of anaerobic fermentation or respiration such as acetate and/or C_1 compounds (CO_2 and hydrogen, formate, CO, methanol, methylamines, and methylsulfides, etc.) are used as the substrates by methanogens. It is estimated that 4% of all net fixed carbon on Earth is remineralized to methane gas in the global carbon cycle (12). In comparison to heterotrophic bacteria such as *Escherichia coli*, methanogens obtain very little ATP for their metabolic lifestyle. *E. coli* aerobically growing on glucose obtains 32 to 38 mol ATP per mole substrate, whereas methanogens obtain between 0.5 to 2 mol ATP per mole substrate, depending on whether they have the ability to synthesize a membrane electron carrier, methanophenazine (MPh) (12, 13).

Most methanogens that have been isolated and characterized are specialists that use CO_2 and hydrogen or formate as the substrates for growth. However, the *Methanosarcinales* order can use a wide array of substrates in addition to CO_2 and formate (12). *Methanosarcina* species, such as *Methanosarcina barkeri* Fusaro, use CO_2 and hydrogen as well as C_1 compounds and acetate to grow. *Methanosarcina acetivorans* C2A is a close relative of *M. barkeri*, but it does not synthesize hydrogenases and is incapable of hydrogenotrophic methanogenesis. Regardless of the substrate, electrons from the reduced electron carriers ferredoxin, deazaflavin F_{420}, or hydrogen gas are used to reduce MPh, a unique membrane-bound electron carrier found so far only in *Methanosarcinales* methanogens (14, 15). MPh has a tricyclic ring phenazine head group and a prenyl tail connected by an ether linkage (Fig. 1a). Reduced MPh is oxidized by the cytochrome-containing terminal oxidoreductase, coenzyme M (CoM)-S-S-coenzyme B (CoB) heterodisulfide reductase, HdrED (Fig. 1b) (14, 16–18). CoM-S-S-CoB is the terminal electron acceptor synthesized in the last step of the methanogenesis pathway (19). The reduction of CoM-S-S-CoB back to the coenzyme M (mercaptoethanesulfonate) and coenzyme B (2-mercaptoheptanoylthreonine phosphate) thiols results in scalar translocation of protons across the cell membrane, similar to a Q-loop mechanism found in organisms that use oxidative respiration (20). However, MPh has a lower redox potential (~ -150 mV for MPh versus -100 or $+100$ mV for quinones), which tailors the methanogen electron transport system to donate electrons to the CoM-S-S-CoB disulfide terminal acceptor (21).

MPh is interesting from an evolutionary perspective, because it is structurally unique yet suggests the selective pressure for the thermodynamic superiority of utilizing a chemiosmotic membrane gradient to conserve energy is ancient (22). We wanted to compare the physiological similarities between MPh synthesized by *Methanosarcina* species and quinones synthesized by bacteria to explore the functional analogy between MPh and quinones (23–25).

RESULTS

Improved methods for methanophenazine extraction and chromatography. If MPh plays the same role in methanogens as quinones do in bacteria, we would expect that MPh should be as abundant in methanogen cell membranes as quinones are in bacteria. To quantify MPh and quinones in genetically tractable *Methanosarcina* strains, we devised a procedure to efficiently extract both species from cell membranes. Careful quantification of MPh in cell membranes requires the use of an internal standard that possesses similar chemical characteristics yet can be distinguished from the molecule under study. It is important that both molecules have similar solvent behaviors to ensure that both molecules are extracted from the crude sample with similar yields.

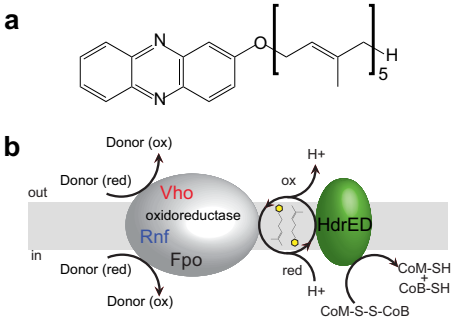

FIG 1 Methanophenazine is a membrane electron carrier in *Methanosarcina*. (a) Structure of methanophenazine (MPh). (b) MPh shuttles electrons between the MPh:CoM-S-S-CoB oxidoreductase HdrED and proton-pumping F_{420}:methanophenazine oxidoreductase (Fpo) or viologen-reducing MPh hydrogenase (Vho) in *M. barkeri*, or between HdrED and Fpo or sodium-pumping ferredoxin:MPh oxidoreductase (Rnf [*Rhodobacter* nitrogen fixation protein]) in *M. acetivorans*.

Taking these considerations into account, we opted to use menaquinone (MK_4) as an internal standard, because it is also a prenylated membrane electron carrier that is not synthesized by methanogen cells and can be commercially purchased (14, 24). To efficiently extract MPh and MK_4, we devised a protocol that uses smaller cell numbers (between 10^7 and 10^8) during small-scale batch growth than previous methods that require extraction from 10 g (dry weight) stationary-phase cells grown in a fermenter, adds hexane extraction, and eliminates an isooctane extraction step as previously described (see Table S1 in the supplemental material) (14). Extracted membrane carriers were then separated by reverse-phase C_{18} column chromatography. The peak eluted after chromatography was collected and confirmed to have a ^{1}H nuclear magnetic resonance imaging (NMR) spectra consistent with the published spectra of MPh extracted from *M. mazei* (see Fig. S1) (14). Our procedure had a mean recovery of the MK_4 internal standard of 89% from technical replicates of exponentially growing and stationary-phase cultures, with a mean variance of 10.8%. The mean variance for MPh from technical replicates was 17% from exponentially growing and 8.9% from stationary-phase cultures, with a mean variance of 14.7% (Table S1).

Methanophenazine from closely related *Methanosarcina* species differs in prenyl saturation. A wide variety of membrane electron carriers are synthesized in nature (26–29). To determine if similar but nonidentical MPh derivatives are synthesized by methanogens, we extracted lipophilic compounds from membranes of genetically tractable *M. acetivorans* and *M. barkeri* (Table 1). Reverse-phase chromatography showed that the elution profile of MPh from *M. acetivorans* is identical to the elution profile of the membrane electron carrier from *M. mazei* (14). However, the membrane electron carrier from *M. barkeri* eluted later, suggesting the membrane electron carrier in *M. barkeri* is slightly more hydrophobic (see Fig. S2) (30). The *M. barkeri* membrane electron carrier had an optical absorbance spectrum identical to that of MPh extracted from *M. acetivorans* (see Fig. S3b and d). As a change in the phenazine head group would be expected to change the optical absorbance spectrum, the difference between MPh in *M. acetivorans* and that in *M. barkeri* is therefore most likely due to a change in the prenyl tail saturation or length (30). To confirm this, MPh extracted from *M. acetivorans* and *M. barkeri* was subjected to liquid chromatography-tandem mass

TABLE 1 Organisms used

NB no.[a]	Organism	Genotype	Reference or source
3	*Escherichia coli* DH5α F′ *lacI*^{q}	F′ *proAB lacI*^{q} Δ*(lacZ)*M15 *zzf*::Tn*10* (Tet^r) *fhuA2*Δ*(argF-lacZ)U169 phoA glnV44* ϕ80Δ*(lacZ)*M15 *gyrA96 recA1 endA1 thi-1 hsdR17*	New England BioLabs
34	*Methanosarcina acetivorans* C2A	Δ*hpt*::ϕC31 *int attP*	59
32	*Methanosarcina barkeri* Fusaro	Δ*hpt*::ϕC31 *int attP*	59

[a]NB no., Buan laboratory strain collection number.

spectrometry (LC-MS/MS) to compare the molecular masses with the published mass for MPh from *M. mazei* (14). As anticipated, MPh from *M. acetivorans* is identical to that from *M. mazei* with a molecular mass of 541 Da (see Fig. S4a). The MPh extracted from *M. barkeri* has an observed molecular mass 2 Da smaller, which exactly matches the mass predicted for an MPh molecule that has only one saturation in the prenyl tail (Fig. S4b). We interpreted these results as an indication that MPh species synthesized by *M. mazei* and *M. acetivorans* have two saturated prenyl moieties on the pentaprenyl tail, whereas that from *M. barkeri* has only one saturated prenyl moiety, confirming the MPh prenyl tail saturation reported by others (31).

Archaea and bacteria adjust the quantity of membrane soluble electron carriers during batch growth. We wanted to determine if methanogens regulate MPh content under conditions of changing substrate availability and population density. To do so, we compared MPh content per cell for *M. acetivorans* and *M. barkeri* incrementally during batch growth. Electron flux through MPh allows *M. acetivorans* to produce a scalar transmembrane ion gradient for ATP synthesis, which results in a higher metabolic efficiency than if electrons were simply donated to a cytoplasmic electron acceptor. Electrons can also flow through the faster albeit non-energy-conserving (nonbifurcating) heterodisulfide reductase (HdrABC) path (32). Therefore, the direction of electron flow through MPh or HdrABC has an effect on the growth rates of the organism and the population as a whole (32, 33).

If MPh synthesis was balanced with cell growth and was independent of population density, the number of MPh molecules per cell would not change regardless of the population density of the cell culture. If membrane carrier synthesis was upregulated, the result would be an increase in the average number of molecules per cell as the number of cells per ml in the culture increases. Conversely, if the cell adjusts energy metabolism in a cell density-dependent manner, then the number of electron carrier molecules per cell would be expected to decrease.

In addition, if the energy conservation mechanism required external diffusion of an electron carrier (such as hydrogen, sulfur compounds, flavins, or phenazines, etc.), the cell runs the risk of losing electrons to nearby competing cells. Because *M. barkeri* uses an obligate hydrogen cycle to conserve energy, at low cell densities during growth on methanol as the sole energy source, electrons are lost as H_2 to the surrounding medium before they can be efficiently captured by MPh-reducing hydrogenase (Vho) (34). Therefore, at low cell densities, cells might be expected to increase MPh pool sizes to maximize the rate of H_2 recapture by hydrogenase at the membrane. At higher cell densities, individual cells will lose electrons through H_2, but a near neighbor in the population could capture the H_2. Likewise, an H_2 molecule(s) from neighboring cells could be captured, and overall, there would be a net zero loss of electrons by the culture population. Accordingly, the *M. barkeri* MPh content per cell could be higher in exponentially growing low-cell-density cultures than in higher-density stationary-phase cultures to compensate for the loss of electrons by H_2 diffusion at a low cell density. *M. acetivorans* would not be expected to exhibit a population-specific MPh synthesis effect, because it does not express functional MPh-dependent hydrogenases ($F_{420}H_2$: MPh oxidoreductase [Fpo] or Vho). Therefore, despite the requirement for MPh by both *M. acetivorans* and *M. barkeri*, the two organisms could regulate MPh synthesis through different mechanisms based on their divergent energy conservation pathways.

We extracted MPh from *M. acetivorans* and *M. barkeri* grown on methanol as the sole carbon and energy sources during batch growth. Under these conditions, *M. acetivorans* and *M. barkeri* have similar growth rates, cell sizes, and shapes. Because *Methanosarcina* can produce gas vacuoles, we related the extracted MPh quantity to cell counts instead of biomass to account for changes in cell density that might occur. In *M. acetivorans* cultures, we observed that the MPh concentration per cell increased 1.67 ± 0.06-fold from the exponential to stationary phase (Fig. 2a). MPh content per cell increased linearly during exponential phase up to 4.10×10^6 molecules per cell and sharply increased as cell counts decreased when cultures reached stationary phase. Therefore, two rates of MPh accumulation were observed, an exponential rate and a

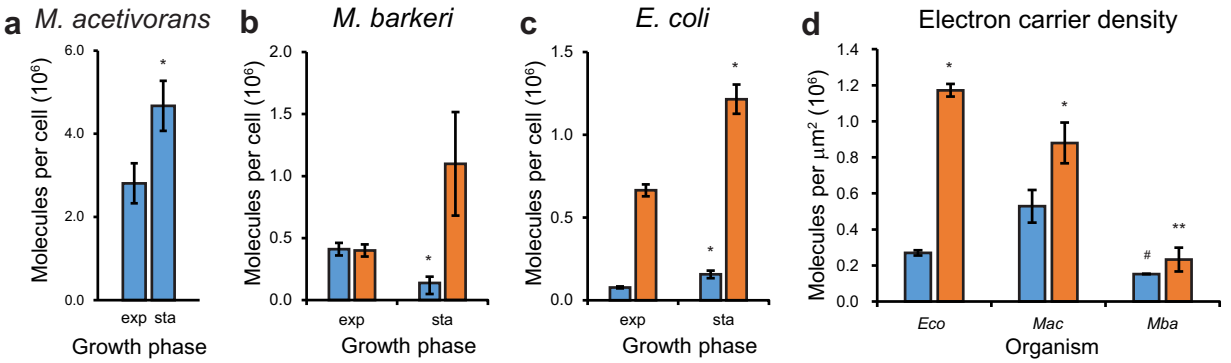

FIG 2 Archaea and bacteria regulate electron carrier density. (a) MPh extracted from *M. acetivorans*. (b) Quantification of monounsaturated (blue bars) and double-saturated MPh (orange bars) in *M. barkeri* cells grown on methanol. (c) Quantification of menaquinone (blue bars) and ubiquinone (orange bars) extracted from *E. coli* cells grown aerobically on LB glucose. (d) Total electron carrier density in cell membranes during exponential (blue bars) or stationary (orange bars) phase. Error bars represent standard deviations. exp, exponential growth phase; sta, stationary-phase cells. *Mac*, *M. acetivorans*; *Mba*, *M. barkeri*; *Eco*, *E. coli*. Student's two-tailed *t* tests: *, $P < 0.01$ versus exponentially growing cells; **, $P < 0.01$ versus stationary-phase *M. acetivorans* cells; #, $P < 0.01$ versus exponentially growing *M. acetivorans* cells.

stationary rate (Fig. 3a). These data indicate that during exponential growth, the rate of MPh synthesis outstrips the rate of cell doubling (Fig. 3b). In stationary phase, the number of cells per ml decreases with time while the molecules of MPh per cell extracted increases. Possible explanations for the increase in MPh concentration per cell as the population stops dividing could be attributed to cell lysis and scavenging or to changing extractability (Fig. 3c). However, we cannot formally exclude the possibility that *M. acetivorans* cells may synthesize MPh at a higher rate in response to entering stationary phase in light of the reasonably good correlation coefficient between cell density and MPh molecules per cell ($R^2 = 0.5215$) (Fig. 3c).

When extracting MPh from *M. barkeri* cultures of different ages, we observed that the total MPh pool did not significantly change as culture turbidity increased, unlike what we observed in *M. acetivorans* cultures (Fig. 2b). Second, we noticed that unlike *M. acetivorans*, *M. barkeri* synthesizes two forms of MPh: a double-saturated form and the historically known monounsaturated form (Fig. 4). In exponential phase, the *M. barkeri* MPh pool is equally composed of double- and monosaturated forms of the electron carrier. However, as cultures enter stationary phase, the representation of each is drastically changed and is instead dominated (93%) by the more reduced double-saturated form of MPh. (Fig. 2b). We did not observe a biphasic increase in MPh content as cells entered stationary phase. Our data suggest *M. barkeri* cells initially produce monosaturated MPh and that prenyl reduction to produce the double-saturated form of MPh may be conditionally regulated.

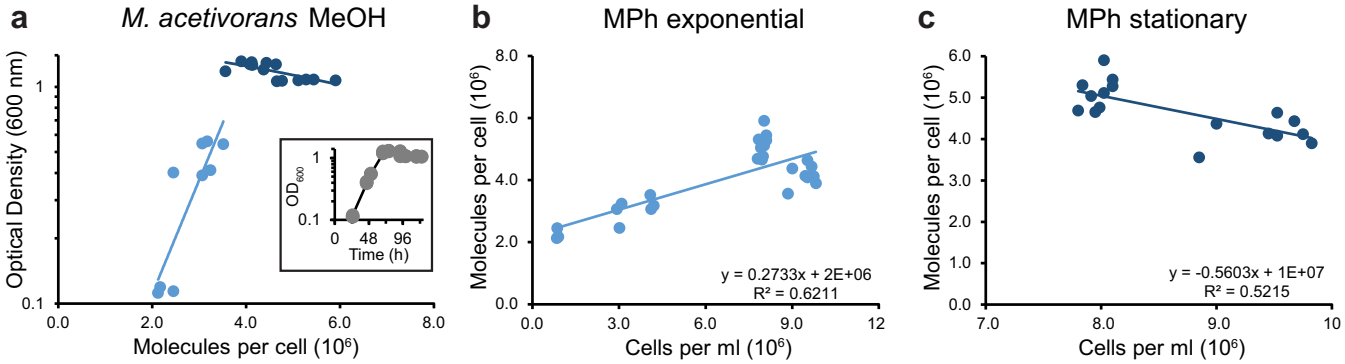

FIG 3 MPh synthesis by *M. acetivorans* during growth on methanol. (a) MPh synthesis is biphasic in *M. acetivorans* cultures (inset, corresponding growth curve). (b) MPh quantity per cell increases linearly with cell density during exponential growth. (c) In stationary phase, as culture density decreases (top right quadrant), MPh quantity per cell increases (top left quadrant).

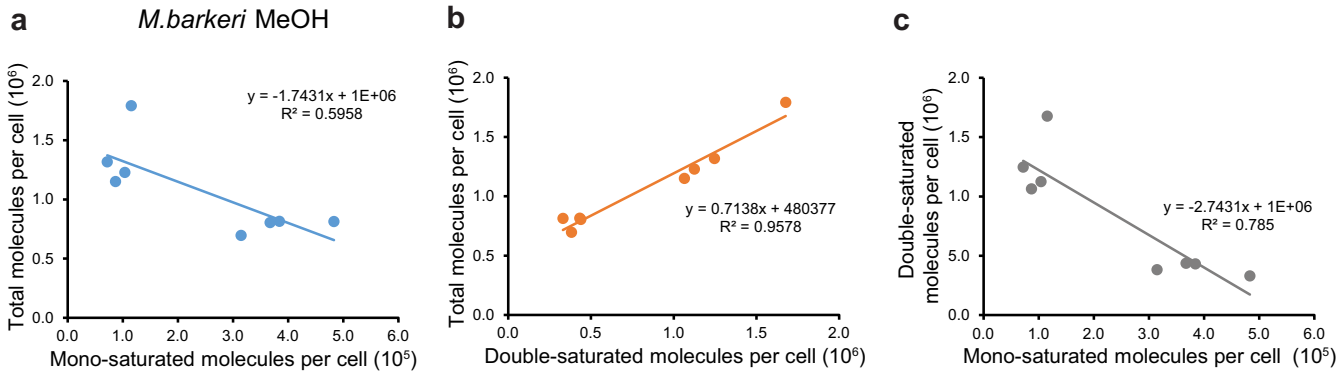

FIG 4 Monounsaturated MPh is reduced to the double-saturated form in *M. barkeri* cells during growth on methanol. (a) Inverse correlation between total and unsaturated MPh quantities in cells. (b) Positive correlation between total and saturated MPh amounts. (c) Inverse correlation between saturated and unsaturated MPh quantities in the cell.

Altogether, these data indicate *M. acetivorans* increases MPh content as the substrate availability decreases and population density increases, while *M. barkeri* keeps the total MPh content steady (though prenyl tail oxidation may be regulated with growth phase). The data support a model of balanced growth and constant MPh synthesis for *M. barkeri* but not for *M. acetivorans*.

Next, we addressed whether our observation of membrane carrier regulation in cultures of *Methanosarcina* species was specific to methane-producing archaea or part of a more general prokaryotic phenomenon. To do so, we quantified membrane electron carriers in *E. coli* bacteria grown aerobically on rich medium supplemented with glucose as the carbon and energy sources and compared the amounts of menaquinone to those of ubiquinone during exponential and stationary phases (35–37). During aerobic exponential growth, *E. coli* synthesizes eight times as much ubiquinone (orange bars) as menaquinone (blue bars), while the total membrane carrier concentration increases 1.85 $\pm$ 0.03-fold from exponential to stationary phase (Fig. 2c). Not only does *E. coli* regulate metabolism by sensing redox states of ubiquinone and menaquinone but the overall electron carrier pool size increases as cultures enter stationary phase, similar to what we observed with methanogen cultures (38). Our data support the idea that some archaea and bacteria increase the amount of electron carriers in their membranes as they transition from exponential to stationary phase growth.

Possibility for isopotential electron tunneling in methanogen membranes. What effect could changing the amount of MPh in the membrane have on cellular energetics? To answer this question, we used the measured dimensions of methanogen and *E. coli* cells to calculate the density of each electron carrier in the membrane. We then arranged the data according to energetics from the most enthalpically driven to the least enthalpically driven (Fig. 2d). In doing so, we noticed a pattern when comparing the relative ratios of quinones and MPh in exponentially growing versus stationary-phase cell populations. Intriguingly, the MPh content profile in *M. acetivorans* was similar to that in *E. coli* cultures grown aerobically on glucose Lysis broth (LB) while *M. barkeri* cells had the lowest average membrane carrier concentration (Fig. 2d).

We then calculated the theoretical rate of isopotential electron tunneling from one reduced MPh (or quinone) to a nearby oxidized electron carrier (Fig. 5a) (39–42). Based on the average number of membrane carrier molecules we measured, it is possible that electrons from one reduced MPh can tunnel to an adjacent MPh in *M. acetivorans* (42). In *M. barkeri*, tunneling may occur in stationary phase but is less probable when cultures are growing exponentially. This can be interpreted to suggest a reduced electron carrier must be physically close to the electron acceptor (such as the terminal oxidase) for electrons to be quickly and efficiently shuttled (Fig. 4b and c). If not, the reduced membrane carrier must diffuse randomly through the membrane until it

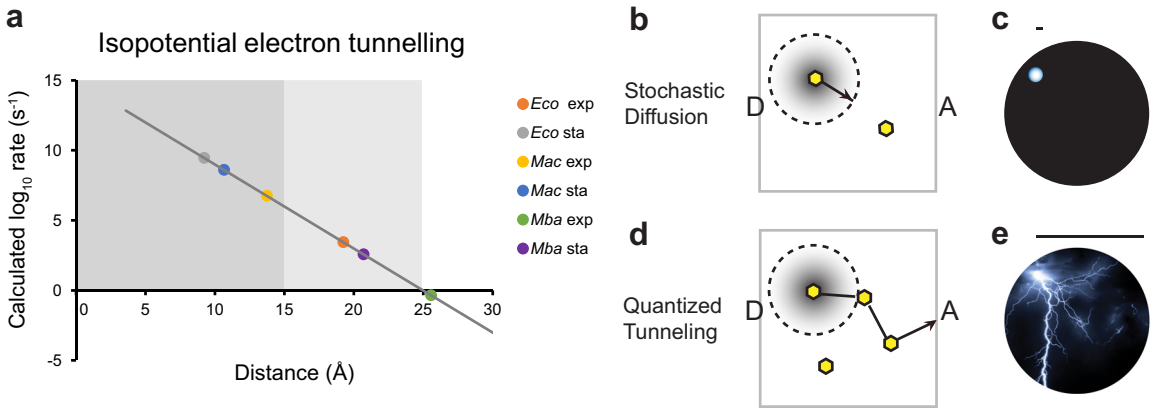

FIG 5 Isopotential electron tunneling in membranes. (a) Total electron carrier concentrations in membranes were used to calculate the theoretical rate of electron transfer for each organism. Dark gray box, rates consistent with quantum tunneling; light gray box, rates where quantum tunneling is possible but less probable. (b) At low electron carrier density (yellow hexagons), electrons must diffuse from the donor (D) to the acceptor (A), resulting in localized electron transfer and slow kinetics. (c) Electrons (white) can diffuse through the membrane (black) to an acceptor within a short radius before decaying to a lower energy state (bar). (d) At high electron carrier density, electrons can tunnel throughout the membrane, resulting in the entanglement of all possible electron donors and acceptors and faster kinetic rates. (e) Electrons (white) can tunnel through the membrane (black) to a more distant acceptor without losing energy (bar). *Eco*, *E. coli*; *Mac*, *M. acetivorans*; *Mba*, *M. barkeri*; exp, exponential growth phase; sta, stationary-phase cells.

comes in close proximity to an acceptor. Any reduced electron carriers that diffuse in the membrane risk either losing the electron to random off-target reactions or a decay in the energy of the electron being transferred. By contrast, for *E. coli* grown aerobically on LB or *M. acetivorans*, regardless of the distance between the electron-donating oxidoreductase and the terminal oxidase, electrons may be able to rapidly tunnel from one membrane carrier to another through the membrane with negligible energy loss until it reaches the terminal oxidase (Fig. 5d and e). Such a situation suggests some *Methanosarcinales* may have electrically "quantized" membranes, in which case the entire membrane could act as one electrically conductive surface, such as a copper metal sheet, rather than a surface studded with individual anode and cathode terminals separated by a nonconductive rubber insulator. Our calculations suggest that in *M. acetivorans*, electrons may be able to tunnel from any one membrane donor to any membrane acceptor at any point on the cell surface through a conductive MPh layer.

We reasoned that if some *Methanosarcinales* have electrically quantized membranes while others do not, the addition of a membrane-soluble (hydrophobic) electron carrier compound with structural and redox properties similar to those of MPh (such as phenazines) to cultures should enhance the growth rate of organisms such as *M. barkeri*, which may not produce an optimal amount of MPh, but will have a modest effect on *M. acetivorans*, which already produces enough MPh to electrically quantize the membrane. Phenazines can be used as extracellular electron shuttles or as toxins that kill cells by generating reactive oxygen species (ROS) that damage proteins and nucleic acids (43, 44). Toxicity in susceptible organisms requires enzymes in the electron transport chain to reduce the phenazines, which then react with molecular oxygen to produce ROS (45). In the experiments we describe, the cells were not exposed to oxygen and remained under strict anaerobic conditions at all times, thus eliminating the possibility of generating hydroxyl radicals from molecular oxygen. Consistent with our prediction, phenazine improved the growth rates and yields for *M. acetivorans* and *M. barkeri*, but the magnitude of the enhancement was more pronounced for *M. barkeri* (Fig. 6). When 10 μM phenazine was added to cultures, the *M. acetivorans* growth rate increased 37% versus a 94% increase in *M. barkeri* cultures (Fig. 6a). Recent reports also show that the addition of phenol red and phenazines to anaerobic digesters and microbial fuel cells does in fact increase the growth of *Methanosarcina* species, demonstrating that this phenomenon is generally relevant to biotechnology (46).

To determine whether hydrophobicity was critical for growth rate enhancement, we tested whether soluble 2-hydroxyphenazine affects the growth of *M. acetivorans*.

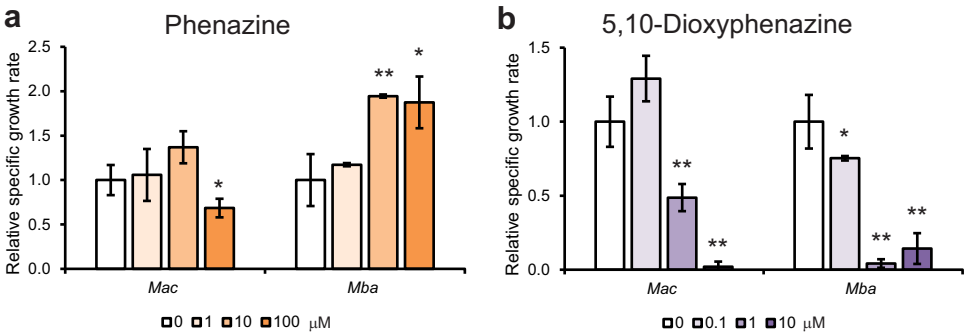

FIG 6 Effects of MPh mimics on growth rate. Increasing concentrations of phenazine (a) or 5,10-dioxyphenazine (b) were added to methanol-grown cultures. *Mac*, *M. acetivorans*; *Mba*, *Methanosarcina barkeri*. Data were collected from six independent cultures per treatment. Error bars represent standard deviations. Student's two-tailed *t* tests versus no added phenazine or 5,10-dioxyphenazine condition: *, $P < 0.05$; **, $P < 0.01$.

2-Hydroxyphenazine closely mimics a hydroxyl moiety in place of the prenyl tail that can be used in place of authentic MPh in MPh H_2:CoM-S-S-CoB heterodisulfide reductase (HdrED) and $F_{420}H_2$:MPh oxidoreductase (Fpo) enzyme assays (15, 18, 47). We expected the more hydrophilic 2-hydroxyphenazine to have a weaker influence on growth than the more hydrophobic phenazine. Consistent with this hypothesis and with other reports, we observed that the addition of 10 μM soluble 2-OH-phenazine did not have an effect on growth rate (data not shown) (18). However, we were able to detect that 2-hydroxyphenazine resulted in a 48.5% decrease in MPh extracted from stationary-phase cultures ($2.38 \pm 0.29 \times 10^6$ molecules per cell versus $4.90 \pm 0.54 \times 10^6$ molecules per cell). This observation, along with our aforementioned results, supports the idea that *M. acetivorans* regulates MPh biosynthesis, though whether the mechanism of regulation is through metabolic, transcriptional, or translational control remains an open question.

We next asked whether the oxidation state of phenazine added to cultures can affect growth. 5,10-Dioxyphenazine is a soluble, fully oxidized phenazine that we expected to inhibit growth by becoming reduced by electrons from the electron transport chain (45). 5,10-Dioxyphenazine has been shown to be a selective hypoxic trigger cytotoxin in human cell lines that is nontoxic when oxidized but produces ROS (hydroxyl radicals) that damage cells when reduced (48). As predicted, despite the lack of molecular oxygen in the medium, 5,10-dioxyphenazine was toxic to both *M. acetivorans* and *M. barkeri* with 50% inhibitory concentrations (IC_{50}s) of 1.4 μM for *M. acetivorans* and 0.2 μM for *M. barkeri* (Fig. 6b). Our results suggest that hydrophobic phenazines, which may be synthetic or naturally produced by bacteria, have the capacity to be reduced by the methanogen electron transport chain (49, 50).

DISCUSSION

For single cells to grow and divide at the maximum rate, the efficiency of electron transfer must surpass the rate of off-target redox reactions and minimize entropic decay through chemical bond vibration and heat dissipation. How have methanogens evolved to minimize energy dissipation while maximizing growth and respiration/fermentation rates? Phylogeny suggests the first methanogens and contemporary obligately hydrogenotrophic methanogens used hydrogen gas to reduce CO_2 or formate and do not use a membrane electron carrier to shuttle electrons from the electron donors (hydrogen and intracellular electron carriers such as deazaflavins F_{420}, FAD, and NAD) to the terminal electron acceptor, CoM-S-S-CoB heterodisulfide (12). Instead, they physically couple the methyl-viologen reducing hydrogenase (Mvh) to the electron-bifurcating terminal oxidase, CoM-S-S-CoB heterodisulfide reductase, HdrABC (51–53). Ergo, the bulk of electron transfer reactions in obligately hydrogenotrophic methanogens occur intracellularly through a network of iron/sulfur clusters and enzyme-bound redox cofactors. *In vivo* protein cross-linking experiments with the obligate hydrog-

enotroph *Methanococcus maripaludis* suggest methanogenesis enzymes form multienzyme complexes that spatially constrain electron donors and enzyme active sites to minimize the relative entropy between methanogenesis pathway steps (51, 53). Forming multienzyme complexes is kinetically and energetically ideal for optimizing any biochemical reactions, and methanogens use the same strategy to maximize growth and metabolism from hydrogen and carbon dioxide.

Methanosarcinales methanogens are postulated to have acquired the ability to use acetate and methylotrophic substrates through lateral gene transfer(s) with *Clostridia* and/or other bacteria (54–56). The ability to use new substrates opened up new trophic niches and allowed the cells to extract more chemical energy for growth but required the cells to find a new way to oxidize the electron carriers. Simply reversing the hydrogenase-catalyzed reactions, while thermodynamically allowable at low hydrogen concentrations, results in the loss of reducing power and makes the cells dependent on establishing a scalar proton transport mechanism to conserve energy.

One solution to the problem of overreduced electron carriers is to evolve and/or acquire hydrogenases and a membrane electron carrier to accelerate scalar proton transport and recapture electrons from hydrogen, resulting in a true hydrogen-cycling mechanism of energy conservation (34, 57). In *Methanosarcinales* such as *M. barkeri* and *Methanosarcina mazei*, MPh is used to couple electrons recaptured from hydrogen by hydrogenases to the HdrED terminal oxidase. Therefore, growth is dependent on the efficiency of recapture of electrons by hydrogenases and the rate that those electrons can be donated to HdrED. In *Methanosarcinales* that do not express hydrogenases, the electron carriers must be balanced by electron transfer through the membrane to generate a proton motive force by scalar proton transport. The MPh step is therefore rate limiting in the central metabolism of methylotrophic substrates or acetate regardless of whether the methanogen expresses hydrogenases (58).

M. acetivorans appears to have maximized the rate of electron transfer through the membrane by synthesizing sufficient amounts of MPh to enable isopotential electron tunneling. We also observed that when growth slows during stationary phase, *M. acetivorans* cells respond by increasing the membrane MPh pool size, which would have the effect of compensating for reduced electron flux by increasing the rate of electron transfer. While the prenyl tail saturation of MPh in *M. barkeri* changes, the total MPh membrane content is constant between cells in exponential and stationary phases. Overall, *M. barkeri* membranes do not contain as much MPh as *M. acetivorans* membranes. How can two closely related *Methanosarcina* species with similar growth rates have such different MPh membrane profiles? Does regulating electron flux through the cell membrane require the regulation of MPh biosynthetic genes to increase MPh pool sizes? Perhaps it does not. There are multiple biophysical strategies that can be employed by cells to modulate the rate of electron transport through the membrane. To maintain efficient electron transfer rates with low contents of electron carriers such as MPh molecules in *M. barkeri* and *M. mazei* and quinones in *E. coli* grown in anaerobic conditions, the cells would need to do one or several things: (i) utilize electron donor and acceptor proteins/enzymes so that each electron carrier molecule has only a short distance to diffuse; (ii) constrain the diffusion of enzyme donors and acceptors by localizing them near each other (such as by forming supramolecular complexes); and/or (iii) express isopotential membrane redox proteins to serve as electrical relays in place of MPh molecules. Depending on the evolutionary pressures and genomic content of a cell lineage, any one (or several) of these strategies could be employed to result in maximal energy conservation efficiency.

MATERIALS AND METHODS

Microorganisms and culture conditions. Organisms were obtained from the sources listed in Table 1 (59). Methanogens were grown in high-salt mineral medium (HS) at 37°C as described previously (60). *Escherichia coli* cells were grown aerobically in 0.5% glucose Lysis broth (LB) with shaking at 37°C (61). 2-OH-phenazine was synthesized *de novo* (62). All other chemicals were obtained from Fisher. Culture growth was measured using a Spectronic D spectrophotometer fitted with a Balch tube (18 mm) modification or using a Tecan Sunrise UV-Vis spectrophotometric plate reader. Cell numbers were

measured microscopically with a Hausmann cell counting chamber using an EVOS FL Auto cell imaging system microscope in the University of Nebraska-Lincoln (UNL) Morrison microscopy core facility. Cell dimensions were measured using NIH ImageJ software (63).

Quinone and methanophenazine extraction. Cells from 100-ml cultures were harvested by centrifugation at 4,000 × *g* for 30 min in a Sorvall Legend XTR tabletop centrifuge fitted with a TX-750 swinging bucket rotor (Thermo Fisher Scientific). Cells were washed with 100 ml of 0.4 M NaCl and resuspended in 1 ml of 0.4 M NaCl. Menaquinone (MK_4) was added as an internal standard (Sigma-Aldrich). The following steps were carried out in the dark to avoid photodegradation. Resuspended cells were lysed by freezing at −80°C 1 h to overnight and then thawing at 37°C in a water bath. Ethanol was added to 70% and the lysates were vortexed and then heated to 70°C for 10 min. Lysates were transferred to glass Hungate tubes and extracted three times with 1 ml hexane. After each addition of hexane, samples were vortexed for 30 s and centrifuged at 2,000 × *g* for 10 min in a TX-750 swinging bucket rotor. Upper hexane organic phases containing MPh and the MK_4 internal standard were combined and transferred to clean Hungate tubes and evaporated under N_2 at 45°C in the dark.

High-performance liquid chromatography. MPh was separated and quantified by reverse-phase high-performance liquid chromatography (HPLC) using an Agilent HPLC system equipped with a UV-Vis detector. Samples were injected into a Supelcosil LC-18 5-μm column (15 cm by 4.6 cm) fitted with a SupelGuard C_{18} guard column (Sigma-Aldrich). Samples were analyzed by isocratic chromatography using either 95% methanol (MeOH) and 5% H_2O or 90% MeOH and 10% hexane mobile phase at 1 ml · min^{-1}. Table S1 in the supplemental material shows the method evaluation of the new MPh extraction procedure with a mobile phase of 90% MeOH and 10% hexane. For quantification of MPh and quinones, absorbances were measured at 255 nm for MPh detection and at 260 nm for quinones (14).

Mass spectrometry. MPh samples were analyzed by LC-MS/MS on an AB SCIEX Q-Trap 4000 integrated mass spectrometer integrated with an Agilent 1200/Dionex U3000 nano LC system in the UNL metabolomics core facility.

Nuclear magnetic resonance imaging. Isolated samples were dissolved in deuterated methanol. Proton NMR data were acquired on a Bruker DRX-500 with a TXI Cryoprobe (500.13 MHz proton frequency). The following data were gathered with a standard 30 degree pulse, 128 scans, and 65,536 data points: ^{1}H NMR(CD_3OD) 8.54 (1.5H, s), 8.21 (d, 1H, J = 8.7 Hz), 8.16 (d, 1H, J = 8.6 Hz), 8.11 (d, 1H, J = 9.3 Hz), 7.91 (t, 1H, J = 8.3 Hz), 7.87 (t, 1H, J = 8.3 Hz), 7.60 (dd, 1H, J = 9.3 and 2.5 Hz), 7.40 (d, 1H, J = 2.6 Hz), 5.14 (t, 1H, J = 7.0 Hz), 5.07 (t, 1H, J = 7.0 Hz), 4.31 (m, 2H), 3.59 (s, 2H), 2.15 to 1.90 (m, 20 H, side chains and impurity), 1.88 (CH_3CN), 1.67 to 1.53 (methyl side chains), 1.28 (impurity, "grease"), and 0.88 (impurity, grease) (64).

SUPPLEMENTAL MATERIAL

Supplemental material for this article may be found at https://doi.org/10.1128/AEM.00950-17.

SUPPLEMENTAL FILE 1, PDF file, 0.6 MB.

ACKNOWLEDGMENTS

This publication was made possible by NIH grant number P20 RR-17675 from the National Center for Research Resources and by the Nebraska Tobacco Settlement Biomedical Research Development Fund. Any opinions, findings, and conclusions or recommendations expressed in this material are those of the author(s) and do not necessarily reflect the views of the funding agencies.

N. R. Buan has disclosed a significant financial interest in RollingCircle Biotech, LLC, and Molecular Trait Evolution, LLC. In accordance with its conflict of interest policy, the University of Nebraska-Lincoln's conflict of interest in research committee has determined that this must be disclosed.

We thank Ryan Grove and Jiri Adamec for assistance with LC/MS, Martha Morton for assistance with NMR, and Raghuveer Singh and Paul Blum for use of HPLC instrumentation.

N. Duszenko carried out experiments and edited the manuscript. N. R. Buan supervised the project, analyzed the data, and wrote and edited the manuscript.

REFERENCES

1. Peck HD, Jr. 1968. Energy-coupling mechanisms in chemolithotrophic bacteria. Annu Rev Microbiol 22:489–518. https://doi.org/10.1146/annurev.mi.22.100168.002421.
2. Harold FM. 1972. Conservation and transformation of energy by bacterial membranes. Bacteriol Rev 36:172–230.
3. Trebst A. 1974. Energy conservation in photosynthetic electron-transport of chloroplasts. Annu Rev Plant Physiol 25:423–458. https://doi.org/10.1146/annurev.pp.25.060174.002231.
4. Thauer RK, Jungermann K, Decker K. 1977. Energy conservation in chemotrophic anaerobic bacteria. Bacteriol Rev 41:100–180.
5. Cobley JG, Cox JC. 1983. Energy conservation in acidophilic bacteria. Microbiol Rev 47:579–595.
6. Poolman B. 1993. Energy transduction in lactic acid bacteria. FEMS Microbiol Rev 12:125–147. https://doi.org/10.1111/j.1574-6976.1993.tb00015.x.
7. Dimroth P, Schink B. 1998. Energy conservation in the decarboxylation of

dicarboxylic acids by fermenting bacteria. Arch Microbiol 170:69–77. https://doi.org/10.1007/s002030050616.
8. Sieber JR, McInerney MJ, Gunsalus RP. 2012. Genomic insights into syntrophy: the paradigm for anaerobic metabolic cooperation. Annu Rev Microbiol 66:429–452. https://doi.org/10.1146/annurev-micro-090110-102844.
9. Buckel W, Thauer RK. 2013. Energy conservation via electron bifurcating ferredoxin reduction and proton/Na(+) translocating ferredoxin oxidation. Biochim Biophys Acta 1827:94–113. https://doi.org/10.1016/j.bbabio.2012.07.002.
10. Schuchmann K, Muller V. 2014. Autotrophy at the thermodynamic limit of life: a model for energy conservation in acetogenic bacteria. Nat Rev Microbiol 12:809–821. https://doi.org/10.1038/nrmicro3365.
11. Wolfe RS. 1971. Microbial formation of methane. Adv Microb Physiol 6:107–146. https://doi.org/10.1016/S0065-2911(08)60068-5.
12. Thauer RK, Kaster AK, Seedorf H, Buckel W, Hedderich R. 2008. Methanogenic archaea: ecologically relevant differences in energy conservation. Nat Rev Microbiol 6:579–591. https://doi.org/10.1038/nrmicro1931.
13. Andersen KB, von Meyenburg K. 1980. Are growth rates of *Escherichia coli* in batch cultures limited by respiration? J Bacteriol 144:114–123.
14. Abken HJ, Tietze M, Brodersen J, Baumer S, Beifuss U, Deppenmeier U. 1998. Isolation and characterization of methanophenazine and function of phenazines in membrane-bound electron transport of *Methanosarcina mazei* Gö1. J Bacteriol 180:2027–2032.
15. Beifuss U, Tietze M, Baumer S, Deppenmeier U. 2000. Methanophenazine: structure, total synthesis, and function of a new cofactor from methanogenic Archaea. Angew Chem Int Ed Engl 39:2470–2472. https://doi.org/10.1002/1521-3773(20000717)39:14<2470::AID-ANIE2470>3.0.CO;2-R.
16. Heiden S, Hedderich R, Setzke E, Thauer RK. 1994. Purification of a two-subunit cytochrome-*b*-containing heterodisulfide reductase from methanol-grown *Methanosarcina barkeri*. Eur J Biochem 221:855–861. https://doi.org/10.1111/j.1432-1033.1994.tb18800.x.
17. Heiden S, Hedderich R, Setzke E, Thauer RK. 1993. Purification of a cytochrome *b* containing H_2:heterodisulfide oxidoreductase complex from membranes of *Methanosarcina barkeri*. Eur J Biochem 213:529–535. https://doi.org/10.1111/j.1432-1033.1993.tb17791.x.
18. Murakami E, Deppenmeier U, Ragsdale SW. 2001. Characterization of the intramolecular electron transfer pathway from 2-hydroxyphenazine to the heterodisulfide reductase from *Methanosarcina thermophila*. J Biol Chem 276:2432–2439. https://doi.org/10.1074/jbc.M004809200.
19. Kunz RC, Dey M, Ragsdale SW. 2008. Characterization of the thioether product formed from the thiolytic cleavage of the alkyl-nickel bond in methyl-coenzyme M reductase. Biochemistry 47:2661–2667. https://doi.org/10.1021/bi701942w.
20. Deppenmeier U. 2004. The membrane-bound electron transport system of *Methanosarcina* species. J Bioenerg Biomembr 36:55–64. https://doi.org/10.1023/B:JOBB.0000019598.64642.97.
21. Tietze M, Beuchle A, Lamla I, Orth N, Dehler M, Greiner G, Beifuss U. 2003. Redox potentials of methanophenazine and CoB-S-S-CoM, factors involved in electron transport in methanogenic archaea. Chembiochem 4:333–335. https://doi.org/10.1002/cbic.200390053.
22. Schoepp-Cothenet B, van Lis R, Atteia A, Baymann F, Capowiez L, Ducluzeau AL, Duval S, ten Brink F, Russell MJ, Nitschke W. 2013. On the universal core of bioenergetics. Biochim Biophys Acta 1827:79–93. https://doi.org/10.1016/j.bbabio.2012.09.005.
23. Shestopalov AI, Bogachev AV, Murtazina RA, Viryasov MB, Skulachev VP. 1997. Aeration-dependent changes in composition of the quinone pool in *Escherichia coli*. Evidence of post-transcriptional regulation of the quinone biosynthesis. FEBS Lett 404:272–274.
24. Alvarez AF, Rodriguez C, Georgellis D. 2013. Ubiquinone and menaquinone electron carriers represent the yin and yang in the redox regulation of the ArcB sensor kinase. J Bacteriol 195:3054–3061. https://doi.org/10.1128/JB.00406-13.
25. Meganathan R. 2001. Biosynthesis of menaquinone (vitamin K2) and ubiquinone (coenzyme Q): a perspective on enzymatic mechanisms. Vitam Horm 61:173–218. https://doi.org/10.1016/S0083-6729(01)61006-9.
26. Udumula V, Endres JL, Harper CN, Jaramillo L, Zhong HA, Bayles KW, Conda-Sheridan M. 2017. Simple synthesis of endophenazine G and other phenazines and their evaluation as anti-methicillin-resistant *Staphylococcus aureus* agents. Eur J Med Chem 125:710–721. https://doi.org/10.1016/j.ejmech.2016.09.079.
27. Garrison AT, Abouelhassan Y, Norwood VM, IV, Kallifidas D, Bai F, Nguyen MT, Rolfe M, Burch GM, Jin S, Luesch H, Huigens RW, III. 2016. Structure-activity relationships of a diverse class of halogenated phenazines that targets persistent, antibiotic-tolerant bacterial biofilms and *Mycobacterium tuberculosis*. J Med Chem 59:3808–3825. https://doi.org/10.1021/acs.jmedchem.5b02004.
28. Ishibashi M. 2014. Bioactive heterocyclic natural products from actinomycetes having effects on cancer-related signaling pathways. Prog Chem Org Nat Prod 99:147–198. https://doi.org/10.1007/978-3-319-04900-7_3.
29. Floss HG. 1997. Natural products derived from unusual variants of the shikimate pathway. Nat Prod Rep 14:433–452. https://doi.org/10.1039/np9971400433.
30. Ogawa T, Yoshimura T, Hemmi H. 2010. Geranylfarnesyl diphosphate synthase from *Methanosarcina mazei*: different role, different evolution. Biochem Biophys Res Commun 393:16–20. https://doi.org/10.1016/j.bbrc.2010.01.063.
31. Elling FJ, Becker KW, Konneke M, Schroder JM, Kellermann MY, Thomm M, Hinrichs KU. 2016. Respiratory quinones in *Archaea*: phylogenetic distribution and application as biomarkers in the marine environment. Environ Microbiol 18:692–707. https://doi.org/10.1111/1462-2920.13086.
32. Catlett JL, Ortiz AM, Buan NR. 2015. Rerouting cellular electron flux to increase the rate of biological methane production. Appl Environ Microbiol 81:6528–6537. https://doi.org/10.1128/AEM.01162-15.
33. Yan Z, Wang M, Ferry JG. 2017. A ferredoxin- and $F_{420}H_2$-dependent, electron-bifurcating, heterodisulfide reductase with homologs in the domains *Bacteria* and *Archaea*. mBio 8:e02285-16. https://doi.org/10.1128/mBio.02285-16.
34. Kulkarni G, Kridelbaugh DM, Guss AM, Metcalf WW. 2009. Hydrogen is a preferred intermediate in the energy-conserving electron transport chain of *Methanosarcina barkeri*. Proc Natl Acad Sci U S A 106:15915–15920. https://doi.org/10.1073/pnas.0905914106.
35. Braun R, Dewey VC, Kidder GW. 1963. On the biosynthesis of the quinone ring of ubiquinone. Biochemistry 2:1070–1072. https://doi.org/10.1021/bi00905a027.
36. Snyder CD, Rapoport H. 1970. Biosynthesis of bacterial menaquinones. Origin of quinone oxygens. Biochemistry 9:2033–2038.
37. Cox GB, Downie JA. 1979. Isolation and characterization of mutants of *Escherichia coli* K-12 affected in oxidative phosphorylation of quinone biosynthesis. Methods Enzymol 56:106–117. https://doi.org/10.1016/0076-6879(79)56013-3.
38. Bekker M, Kramer G, Hartog AF, Wagner MJ, de Koster CG, Hellingwerf KJ, de Mattos MJ. 2007. Changes in the redox state and composition of the quinone pool of *Escherichia coli* during aerobic batch-culture growth. Microbiology 153:1974–1980. https://doi.org/10.1099/mic.0.2007/006098-0.
39. Page CC, Moser CC, Chen X, Dutton PL. 1999. Natural engineering principles of electron tunnelling in biological oxidation-reduction. Nature 402:47–52. https://doi.org/10.1038/46972.
40. Santabarbara S, Heathcote P, Evans MC. 2005. Modelling of the electron transfer reactions in photosystem I by electron tunnelling theory: the phylloquinones bound to the PsaA and the PsaB reaction centre subunits of PS I are almost isoenergetic to the iron-sulfur cluster F(X). Biochim Biophys Acta 1708:283–310. https://doi.org/10.1016/j.bbabio.2005.05.001.
41. Osyczka A, Moser CC, Daldal F, Dutton PL. 2004. Reversible redox energy coupling in electron transfer chains. Nature 427:607–612. https://doi.org/10.1038/nature02242.
42. Gu PY, Zhao Y, He JH, Zhang J, Wang C, Xu QF, Lu JM, Sun XW, Zhang Q. 2015. Synthesis, physical properties, and light-emitting diode performance of phenazine-based derivatives with three, five, and nine fused six-membered rings. J Org Chem 80:3030–3035. https://doi.org/10.1021/jo5027707.
43. Pierson LS, III, Pierson EA. 2010. Metabolism and function of phenazines in bacteria: impacts on the behavior of bacteria in the environment and biotechnological processes. Appl Microbiol Biotechnol 86:1659–1670. https://doi.org/10.1007/s00253-010-2509-3.
44. Hernandez ME, Kappler A, Newman DK. 2004. Phenazines and other redox-active antibiotics promote microbial mineral reduction. Appl Environ Microbiol 70:921–928. https://doi.org/10.1128/AEM.70.2.921-928.2004.
45. Hassett DJ, Charniga L, Bean K, Ohman DE, Cohen MS. 1992. Response of *Pseudomonas aeruginosa* to pyocyanin: mechanisms of resistance, antioxidant defenses, and demonstration of a manganese-cofactored superoxide dismutase. Infect Immun 60:328–336.
46. Beckmann S, Welte C, Li XM, Oo YM, Kroeninger L, Heo Y, Zhang MM, Ribeiro D, Lee M, Bhadbhade M, Marjo CE, Seidel J, Deppenmeier U,

Manefield M. 2016. Novel phenazine crystals enable direct electron transfer to methanogens in anaerobic digestion by redox potential modulation. Energy Environ Sci 9:644–655. https://doi.org/10.1039/C5EE03085D.
47. Baumer S, Ide T, Jacobi C, Johann A, Gottschalk G, Deppenmeier U. 2000. The $F_{420}H_2$ dehydrogenase from *Methanosarcina mazei* is a redox-driven proton pump closely related to NADH dehydrogenases. J Biol Chem 275:17968–17973. https://doi.org/10.1074/jbc.M000650200.
48. Cerecetto H, Gonzalez M, Lavaggi ML, Azqueta A, Lopez de Cerain A, Monge A. 2005. Phenazine 5,10-dioxide derivatives as hypoxic selective cytotoxins. J Med Chem 48:21–23. https://doi.org/10.1021/jm0492150.
49. Rabaey K, Boon N, Hofte M, Verstraete W. 2005. Microbial phenazine production enhances electron transfer in biofuel cells. Environ Sci Technol 39:3401–3408. https://doi.org/10.1021/es048563o.
50. Park DH, Zeikus JG. 2000. Electricity generation in microbial fuel cells using neutral red as an electronophore. Appl Environ Microbiol 66:1292–1297. https://doi.org/10.1128/AEM.66.4.1292-1297.2000.
51. Costa KC, Lie TJ, Xia Q, Leigh JA. 2013. VhuD facilitates electron flow from H_2 or formate to heterodisulfide reductase in *Methanococcus maripaludis*. J Bacteriol 195:5160–5165. https://doi.org/10.1128/JB.00895-13.
52. Kaster AK, Moll J, Parey K, Thauer RK. 2011. Coupling of ferredoxin and heterodisulfide reduction via electron bifurcation in hydrogenotrophic methanogenic archaea. Proc Natl Acad Sci U S A 108:2981–2986. https://doi.org/10.1073/pnas.1016761108.
53. Costa KC, Wong PM, Wang T, Lie TJ, Dodsworth JA, Swanson I, Burn JA, Hackett M, Leigh JA. 2010. Protein complexing in a methanogen suggests electron bifurcation and electron delivery from formate to heterodisulfide reductase. Proc Natl Acad Sci U S A 107:11050–11055. https://doi.org/10.1073/pnas.1003653107.
54. Suharti S, Wang M, de Vries S, Ferry JG. 2014. Characterization of the RnfB and RnfG subunits of the Rnf complex from the archaeon *Methanosarcina acetivorans*. PLoS One 9:e97966. https://doi.org/10.1371/journal.pone.0097966.
55. López-Garcia P, Zivanovic Y, Deschamps P, Moreira D. 2015. Bacterial gene import and mesophilic adaptation in archaea. Nat Rev Microbiol 13:447–456. https://doi.org/10.1038/nrmicro3485.
56. Nitschke W, Russell MJ. 2013. Beating the acetyl coenzyme A-pathway to the origin of life. Philos Trans R Soc Lond B Biol Sci 368:20120258. https://doi.org/10.1098/rstb.2012.0258.
57. Odom JM, Peck HD, Jr. 1984. Hydrogenase, electron-transfer proteins, and energy coupling in the sulfate-reducing bacteria *Desulfovibrio*. Annu Rev Microbiol 38:551–592. https://doi.org/10.1146/annurev.mi.38.100184.003003.
58. Buan NR, Metcalf WW. 2010. Methanogenesis by *Methanosarcina acetivorans* involves two structurally and functionally distinct classes of heterodisulfide reductase. Mol Microbiol 75:843–853. https://doi.org/10.1111/j.1365-2958.2009.06990.x.
59. Guss AM, Rother M, Zhang JK, Kulkarni G, Metcalf WW. 2008. New methods for tightly regulated gene expression and highly efficient chromosomal integration of cloned genes for *Methanosarcina species*. Archaea 2:193–203. https://doi.org/10.1155/2008/534081.
60. Metcalf WW, Zhang JK, Shi X, Wolfe RS. 1996. Molecular, genetic, and biochemical characterization of the *serC* gene of *Methanosarcina barkeri* Fusaro. J Bacteriol 178:5797–5802. https://doi.org/10.1128/jb.178.19.5797-5802.1996.
61. Uetake H, Luria SE, Burrous JW. 1958. Conversion of somatic antigens in *Salmonella* by phage infection leading to lysis or lysogeny. Virology 5:68–91. https://doi.org/10.1016/0042-6822(58)90006-0.
62. Tietze M, Iglesias A, Merisor E, Conrad J, Klaiber I, Beifuss U. 2005. Efficient methods for the synthesis of 2-hydroxyphenazine based on the Pd-catalyzed N-arylation of aryl bromides. Org Lett 7:1549–1552. https://doi.org/10.1021/ol050198y.
63. Girish V, Vijayalakshmi A. 2004. Affordable image analysis using NIH Image/ImageJ. Indian J Cancer 41:47.
64. Gottlieb HE, Kotlyar V, Nudelman A. 1997. NMR chemical shifts of common laboratory solvents as trace impurities. J Org Chem 62:7512–7515. https://doi.org/10.1021/jo971176v.